

Central Lancashire Online Knowledge (CLoK)

Title	Fabricating a Shell-Core Delayed Release Tablet Using Dual FDM 3D Printing for Patient-Centred Therapy
Type	Article
URL	https://clock.uclan.ac.uk/16486/
DOI	https://doi.org/10.1007/s11095-016-2073-3
Date	2017
Citation	Okwuosa, Tochukwu Chijioke, Carrapico-Pereira, Beatriz, Arafat, Basel, Cieszynska, Milena, Isreb, Abdullah and Albed Alhnan, Mohamed (2017) Fabricating a Shell-Core Delayed Release Tablet Using Dual FDM 3D Printing for Patient-Centred Therapy. <i>Pharmaceutical Research</i> , 34 (2). pp. 427-437. ISSN 0724-8741
Creators	Okwuosa, Tochukwu Chijioke, Carrapico-Pereira, Beatriz, Arafat, Basel, Cieszynska, Milena, Isreb, Abdullah and Albed Alhnan, Mohamed

It is advisable to refer to the publisher's version if you intend to cite from the work.
<https://doi.org/10.1007/s11095-016-2073-3>

For information about Research at UCLan please go to <http://www.uclan.ac.uk/research/>

All outputs in CLoK are protected by Intellectual Property Rights law, including Copyright law. Copyright, IPR and Moral Rights for the works on this site are retained by the individual authors and/or other copyright owners. Terms and conditions for use of this material are defined in the <http://clock.uclan.ac.uk/policies/>

Fabricating a Shell-Core Delayed Release Tablet Using Dual FDM 3D Printing for Patient-Centred Therapy

Tochukwu C Okwuosa¹, Beatriz C Pereira¹, Basel Arafat¹, Milena Cieszynska¹, Abdullah Isreb¹, Mohamed A Alhnan^{1*}

¹ School of Pharmacy and Biomedical Sciences, University of Central Lancashire, Preston, Lancashire, UK

*Corresponding author: MAIbedAlhnan@uclan.ac.uk

ABSTRACT

Purpose. Individualizing gastric-resistant tablets is associated with major challenges for clinical staff in hospitals and healthcare centres. This work aims to fabricate gastric-resistant 3D printed tablets using dual FDM 3D printing.

Methods. The gastric-resistant tablets were engineered by employing a range of shell-core designs using polyvinylpyrrolidone (PVP) and methacrylic acid co-polymer for core and shell structures respectively. Filaments for both core and shell were compounded using a twin-screw hot-melt extruder (HME). CAD software was utilized to design a capsule-shaped core with a complementary shell of increasing thicknesses (0.17, 0.35, 0.52, 0.70 or 0.87 mm). The physical form of the drug and its integrity following an FDM 3D printing were assessed using x-ray powder diffractometry (XRPD), thermal analysis and HPLC.

Results. A shell thickness ≥ 0.52 mm was deemed necessary in order to achieve sufficient core protection in the acid medium. The technology proved viable for incorporating different drug candidates; theophylline, budesonide and diclofenac sodium. XRPD indicated the presence of theophylline as crystals whilst budesonide and diclofenac sodium remained in the amorphous form in the PVP matrix of the filaments and 3D printed tablets. Fabricated tablets demonstrated gastric resistant properties and a pH responsive drug release pattern in both phosphate and bicarbonate buffers.

Conclusions. Despite its relatively limited resolution, FDM 3D printing proved to be a suitable platform for a single-process fabrication of delayed release tablets. This work reveals the potential of dual FDM 3D printing as a unique platform for personalising delayed release tablets to suit an individual patient's needs.

KEYWORDS: *Delayed release; gastric resistant; modified-release, personalised; patient-specific; additive manufacturing*

ABBREVIATIONS

API	active pharmaceutical ingredient
CAD	computer aided design
DSC	differential scanning calorimetry
FDM	Fused Deposition Modelling
HME	hot melt extrusion
HPLC	high performance liquid chromatography
MTDSC	modulated temperature differential scanning calorimetry
PEG	polyethylene glycol
PVP	polyvinylpyrrolidone
SEM	scanning electron microscopy
TBP	tribasic sodium phosphate
TEC	triethyl citrate
T _g	glass transition temperature
T _m	melting point
TGA	thermal gravimetric analysis
XRPD	X-ray powder diffractometry

INTRODUCTION

Latest advances in pharmacogenomics and clinical trials have put more emphasis on individualizing treatment in a patient-centred health care (1). One important aspect of personalizing treatment is individualizing dosage forms. In case of solid dosage forms, dose personalisation by splitting of tablets has been associated with dose variation (2, 3). Moreover, the splitting of coated tablets physically compromises the barrier function of the coating, rendering dose adjustment impractical for delayed and modified release tablets (4). One potential solution for personalising the dose of solid dosage forms is the on-demand manufacturing by using a benchtop 3D printer (5). This approach offers several advantages to both healthcare workers and patients, such as flexibility in modifying the dose, shape and size of the dosage form in response to patient's or healthcare staff's needs (6). Therefore, it would be of great interest to fabricate an enteric dosage using a bench-top 3D printer.

Enteric coated formulations are produced by carrying out two main steps; i) production of an API-loaded core, and ii) coating the core with synthesized or semi-synthesized polymers (7, 8). The technology requires paradoxical criteria of no or limited drug release in the acid media followed by the release of 80 % of the actives in the intestinal phase within a certain time limit (9). These criteria are usually met by applying a 30-100 µm thick film to a core (e.g. tablets, pellets). However, achieving such a demanding criteria via 3D printing technologies creates some major technical challenges such as i) grafting a consistent protective shell within the resolution of 3D printers, ii) achieving adhesion and compatibility between the shell and core materials, and iii) coordinating simultaneous applications of the shell and core materials.

These challenges were reflected by the absence of literature reports utilizing 3D printing technologies for the fabrication of delayed release shell-core tablets. Although powder based 3D printing have been reported for immediate and controlled release (10-12), no examples of delayed release tablets meeting the pharmacopeial criteria have been reported. Yet, one relevant attempt was the use of TheriForm technology (powder-based 3D printing) to manufacture a dual pulsatile release system composed of 3 chambers (11, 13). In the enteric chamber, an ethanolic solution of the enteric polymer was sprayed onto a mixture of lactose and MMC, resulting in a pH dependent behaviour and a drug release over 4 h in the intestinal phase.

With increased interest in FDM 3D printing in fabrication of oral tablets for extended (5, 14-16) and immediate drug release (17-19), few attempts have been reported utilising the technology for enteric tablets. For instance, FDM 3D printed PVA based tablets were coated with methacrylic polymer to target the colon using a conventional fluidized bed coater (20). More recently, a double disc containing an enteric layer was fabricated by FDM 3D printing and the drug release from the disc was assessed using a test cell assembly (21). As far as the authors know, there have been no previous examples of complete production of delayed release tablets through 3D printing.

Recent technological advances have made 3D printers available with multiple nozzles. Such advances paved its way in artistic designs (22, 23), the manufacturing of composite elements (24), as well as pharmaceutical applications (25). In this effort, we aim to fabricate an enteric coated tablet using a dual-nozzle single step FDM 3D printing process. The gastric-resistant tablets were engineered by employing a range of shell-core designs using polyvinylpyrrolidone (PVP) and methacrylic acid copolymer for core and shell structures respectively, such polymers have been also broadly exploited in supporting other advance techniques (26, 27) . Theophylline was used initially as a model drug for its thermal stability, small molecular weight and high water solubility, rendering it an ideal model drug to test the efficiency of controlling drug release from the enteric system. Later, other model drugs commonly available as gastric-resistant products (budesonide and sodium diclofenac) were deployed in this system.

MATERIALS AND METHODS

Materials

Theophylline was purchased from Acros Organics (UK). Polyvinylpyrrolidone (PVP, MW 40,000), PEG400, castor oil, triethyl citrate, tribasic phosphate (TBP) and oleic acid and dipyrindamole were purchased from Sigma-Aldrich (UK). Talc was ordered from Fluka Analytical (UK). Scotch blue painter's tape 50 mm was supplied by 3M (Bracknell, UK). Eudragit L100-55 was donated by Evonik Industries (Darmstadt, Germany).

Preparation of filaments using HME

For the preparation of the core filaments, a Thermo Scientific HAAKE MiniCTW hot melt extruder (Karlsruhe, Germany) was utilised. An optimised ratio of a powder mixture constituting of the polymer (PVP), plasticizer (TEC), filler (talc) or tribasic phosphate sodium (TBP) and API (theophylline) respectively (Table I) was adapted from previous work (18). The mixture was gradually added to the HME and allowed to mix for 5 min at 100 °C to allow homogenous distribution of the molten mass. Afterwards, extrusion took place at 90 °C at a torque of 0.4 Nm and 1.25 mm nozzle size. Optimised filaments were also modified to include another two model drugs, budesonide (2.3%wt) and diclofenac sodium (20%wt). The change in drug concentration allowed achieving a representative dose for budesonide (3 mg) and diclofenac sodium (25 mg) from the model core. For the preparation of the shell, Eudragit L100-55, TEC and talc (50, 16.67 and 33.33%wt) were mixed at 135 °C for 5 min in a HME and extruded at 125 °C using 1 mm nozzle size.

Tablet design and printing

The core-shell tablets were designed in a caplet shape as described in a previous study (18). In order to assess the impact of shell thickness, a number of designs with increasing shell thicknesses (0.17, 0.35, 0.52, 0.70 or 0.87mm) were constructed. All the shell designs were complementary to the same core. Shell-core tablets were printed using modified settings of the software: Shell and core printing temperatures were 185 °C and 110 °C respectively and the platform was heated to 40 °C. The first layer, infill, inset and outline layers were printed at 12 mm/s extrusion speed and 50 mm/s travelling speed. The resolution was set as standard (200 µm layer thickness).

In a separate experiment and in order to assess the impact of 3D printing resolution, the resolution of core-shell theophylline tablet with 0.52mm were printed at low, standard and high resolutions.

Thermal analysis

For modulated temperature differential scanning calorimetry (MTDSC) analysis, a differential scanning calorimeter (DSC) Q2000 (TA Instruments, Elstree, Hertfordshire, UK) was employed, using previously reported method in an earlier study (18). In order to assess the impact of different lubricant on thermal stability of the PVP filament, TGA analysis was employed as previously specified (18).

X-ray Powder diffractometry (XPRD)

The physical form of model APIs in PVP, PVP: TEC filament, API-free and API-loaded filaments, and 3D printed tablets were assessed using a powder X-ray diffractometer, D2 Phaser with Lynxeye (Bruker, Germany). Samples were scanned from 2Theta (2θ)= 5° to 50° using the parameters as previously reported (18).

Determination of drug content

In order to examine the effect of HME and FDM 3D printing on the integrity of API, API-loaded filaments and 3D printed tablets were analysed for drug content prior and following HME as well as in the 3D printed tablets. Samples (API loaded filaments or tablets) were accurately weighed and placed in a 500 mL of 0.1N HCl, 1:1 water: acetonitrile mixture or phosphate buffer 6.8 for 2 h under sonication for theophylline, budesonide and diclofenac sodium respectively. The solutions were filtered through 0.22 μ m Millex-GP syringe filters (Merck Millipore, USA) and prepared for HPLC analysis.

Theophylline content in relevant samples was assessed using an Agilent UV-HPLC 1260 series (Agilent Technologies, Inc., Germany) equipped with XTerra RP 18 column (150 \times 4.6 mm, 5 μ m particle size) (Waters, Ireland) at a temperature of 40°C. The mobile phase consists of a 10 mM solution of ammonium acetate buffer, methanol and acetonitrile (86:7:7). Analysis was carried out at a wavelength of 272 nm, flow rate of 1 mL/min, injection volume was 5 μ L and a run time of 7 min.

Budesonide content was assessed using an Agilent UV-HPLC 1260 series (Agilent Technologies, Inc., Germany) equipped with synergy max column at 30°C. A mixture of acetonitrile and pH 3 water (55:45) was used as a mobile phase. Analysis was carried out at a wavelength of 244 nm, flow rate of 1.5 mL/min, injection volume was 50 µL and a run time of 10 min.

For diclofenac sodium, samples were assessed using an Agilent UV-HPLC 1200 series (Agilent Technologies, Inc., Germany) equipped with synergy fusion column at temperature 30°C. The mobile phase was made up of methanol and pH 2 water (80:20). Analysis was carried out at a wavelength of 280 nm, flow rate of 1 mL/min, injection volume was 10 µL and a run time of 10 min.

Scanning electron microscopy (SEM)

Quanta-200 SEM microscope at 20 kV was used to examine the surface morphology of the printed shell-core structures. Samples were placed on a metallic stub and then gold coated under vacuum using JFC-1200 Fine Coater (Jeol, Tokyo, Japan). Images of the tablets were also taken using a Canon EOS-1D Mark IV (Canon Ltd, Japan).

Raman Spectroscopy

Raman spectroscopy (Horiba HR800, UK) was used to analyse and map the flat surface of the content of a 50% printed tablet. A green laser was used (532nm) with 25% filter and 600 grating. The slit and hole were set to 100 and 300 µm respectively. An acquisition time of 2 sec was used with an accumulation of 5 scans per point. Samples were scanned from 1200 nm to 1800 nm with a step size of 150 µm. The band for theophylline was assigned a red colour, whilst a green colour was assigned to Eudragit L100-55. Labspec 6 spectroscopy software suite (Horiba Scientific, Japan) was used to process the data.

***In vitro* disintegration and dissolution studies**

a. Disintegration tests. Disintegration studies were conducted following United States Pharmacopeia 30 standards (9). Six tablets were placed in the baskets of DT700 disintegration apparatus (Erweka, Germany) and were shaken for an hour in 0.1M HCl. The gastric medium was then replaced with phosphate buffer pH 6.8. The

experiment was continued and the time for complete disintegration of all tablets was recorded.

b. Acid uptake tests. In order to assess the ability of the 3D printed enteric shell to protect the core, three coated tablets were weighed individually prior to 2-hours exposure to 0.1M HCl at 37 °C. The tablets were then drained off the acidic medium, dried with filter paper and weighted again. The acid uptake was calculated as follows:

$$\text{Weight gain (\%)} = \frac{\text{wet mass} - \text{dry mass}}{\text{dry mass}} \times 100$$

c. pH change dissolution test (phosphate buffer). *In vitro* drug release studies for all gastro-resistant tablets used in this study were conducted using an AT 7 Smart dissolution USP II apparatus (Sotax, Switzerland). Each experiment was carried out in triplicate in dissolution medium at 37±0.5 °C with a paddle speed of 50 rpm. The tablets were tested in 750 mL of a stimulated gastric fluid (0.1M HCl, pH 1.2) for 2 h, followed by 4-h exposure to pH 6.8 phosphate buffer.

Within all the experiment the amount of released theophylline was determined at 5 min intervals by UV/VIS spectrophotometer (PG Instruments Limited, UK) at a wavelength of 272 nm and path length of 1 mm. Data was analysed using IDISis software (Automated Lab, 2012). For budesonide and diclofenac sodium, samples (2 mL) were manually collected at 0, 15, 30, 60, 90, 120, 150, 165, 180, 210, 240, 300, 360, 420 and 480 min. They were then assessed using the HPLC methods outlined in the HPLC method described in section 2.5.

d. pH change dissolution test (bicarbonate buffer). In order to assess the drug release pattern in a more physiologically relevant medium, an additional evaluation of drug release was performed in pH 7.4 modified Krebs bicarbonate buffer. The latter better simulates the buffer capacity, pH and ionic composition of human gastric fluids (28).

The dissolution test was carried out following the same protocol specified in section 2.8c. For the first 2 hours, tablets were exposed to 900 mL of 0.1 HCl (pH 1.2). Tablets were then retrieved from the acidic medium and introduced into 900 mL of modified

Krebs buffer for an additional 4 h (1.18 mM KH_2PO_4 , 24 mM NaHCO_3 , 118.07 mM NaCl , 4.69 mM KCl , 2.52 mM CaCl_2 , and 1.18 mM $\text{MgSO}_4 \cdot 7\text{H}_2\text{O}$).

Statistical analysis

One-way ANOVA was employed using SPSS Software (22.0.0.2) to analyse the results. Differences in results of $p < 0.05$ were considered to be significant.

RESULTS AND DISCUSSION

Fig.1 provides a schematic illustration of the fabrication of 3D-printed shell-core enteric tablets. CAD software was utilized to design two complementary stereolithographic files to form a shell-core structure. Dual FDM 3D printer was employed with two different filaments; i) filament for enteric shell (Eudragit L100-55), and ii) filament for the core (API, PVP) processed through an HME compounder. Theophylline was used as a model drug to develop the enteric core structure due to its high solubility in acidic medium and small molecular weight, rendering it a major challenge for an enteric system (29).

Unlike single FDM 3D printing of theophylline (18), frequent blocking of PVP filament (core) was encountered in dual FDM 3D printing. It is possible that whilst the first nozzle is printing, the filament in the second head remains at elevated temperature leading to material adherence to the inner wall of the nozzle head. To overcome the blocking of the nozzle, several additives were initially incorporated in PVP filament composition. However, it led to the softening of the filament and rendered it incompatible with the gear of the 3D printer. An alternative solution inspected was the addition of lubricant liquids with high boiling points (castor oil, oleic acid or PEG 400). All three liquids allowed successful printing of tablets without affecting the TGA patterns of the polymer (Supplementary Data, Fig. S1A) or the dissolution rate of theophylline from the filaments (Supplementary Data, Fig. S1B). It is likely that these liquids exhibit a lubricating rather than protective effect and physically prevents the sticking of the filament to the internal wall of the nozzle, hence allowing smooth alternation between nozzles. Based on these findings it was decided to choose one lubricant, oleic acid to facilitate dual 3D printing.

Following the optimisation of the core matrix, it was possible to graft a shell material based on developing a filament comprising of Eudragit L100-55, TEC and talc at a ratio of: 50, 16.67 and 33.33%wt, respectively. Eudragit L100-55 is a methacrylic acid-ethyl acrylate copolymer (1:1) commonly used for the preparation of enteric solid dosage forms. Its unique structure gives it an enteric pH-dependent character, being insoluble at physiological pH values and soluble above pH 5.5 medium (30). The used ratio was deemed necessary to significantly lower the T_g of Eudragit L100-55 from 125.53 °C to 10.23 °C (Supplementary Data, Fig. S2) to allow continuous flow from

FDM 3D printer's nozzle, whilst solidifying quickly to permit the formation of a well-defined structure.

In order to adjust the pH response release pattern of core-shell structures, tablets with identical cores comprising theophylline as a model drug were fabricated with increasing thicknesses of the Eudragit L100-55 shell (Fig. 2A-D). *In vitro* dissolution tests indicated that thickness levels 0.17 and 0.35 mm led to a premature release of the drug in the acidic medium (Fig. 2E). It is possible that these thicknesses only allowed the printing of 1-2 layers in the shell structure, which was insufficient to control drug release. When a thicker shell design was applied (0.52, 0.7 or 0.87 mm), a superior control of drug release was achieved (<3% of drug released after 120min in gastric medium). This was accompanied with the formation of larger number of layers (3-5 layers), which is essential to construct a gastric-resistant barrier to the acidic medium. It is notable the drug release in the intestinal phase (pH 6.8) followed a bi-phase pattern; a relatively slow drug release in the initial 45 min after pH change followed by a faster release after 45 min. It is possible that the first phase reflects the diffusion of the model drug through the eroding enteric shell layers, whilst a faster release takes place following the complete dissolution of the shell, where a water-soluble PVP-based core starts to dissolve. Such a pattern has been seen in shell-core structures (25), where erosion of the external layer preceded the dissolution of the core.

The impact of FDM 3D printing resolution (layer thickness) on the dissolution of shell-core structures was also investigated using 0.52mm shell (Fig. 3A). Reducing the resolution of the 3D printing (reducing number of layers to fabricate the shell) in low and standard resolutions resulted in a relatively slower response to pH change in comparison to high resolution (Fig. 3B). It is worthy to note that using FDM 3D printing, a much thicker shell layer was needed to achieve sufficient gastric resistant pattern in comparison to conventionally coated tablets with fluid-bed or pan coater (30-100 μm) (31) which reflects the difficulty of producing a complete protective layer with a single layer of filament.

In order to accelerate drug release in the intestinal phase, an alkalinizing agent, tribasic phosphate sodium (TBP), was examined as a filler in a replacement for talc. The strategy allowed a much faster dissolution pattern in the intestinal phase (Fig. 3C),

it is likely that TBP in the core would dissolve with water imbibition upon pH change, leading to a rise in the local pH resulting in acceleration of dissolution of Eudragit L100-55 shell and hence faster release of the API (32). However, the use of TBP was associated with a drop in weight as revealed by TGA (Supplementary Data, Fig. S3). HPLC analysis confirmed a significant drop in drug content (86%) (Table I). These findings suggest that, unlike talc which acts as an inert filler, TBP tends to react with theophylline at an elevated temperature leading to a significant drug degradation. Hence, talc was considered as the filler of choice for this study.

Raman spectral mapping was utilised to generate a detailed chemical image of the flat surface of a 50% complete 3D printed tablet (Fig. 3D1). Interrogation of individual spectra to produce false colour representations of distribution for theophylline (green) and Eudragit L100-55 (red) elucidated a definitive separation between the core and the shell (Fig. 3D2), suggesting the presence of theophylline in the core of the tablet with no signs of it diffusing into the Eudragit L100-55 shell.

In order to prove the suitability of the system to different APIs, two other model drugs, budesonide or diclofenac sodium, were also examined by including them individually in the PVP based filament. TGA thermographs (Figs. 4A-B) showed a mass drop of PVP filaments around 100 °C due to water loss whilst a second major mass drop was also apparent at 400 °C due to the degradation of PVP. The thermal stability of both model APIs, similar to earlier studies, showed no further weight loss at temperatures <200 °C for budesonide (20) and diclofenac sodium (33).

Analogous to TGA results, DSC thermographs of PVP displayed a large endothermic event in the range of 50-110 °C due to polymer dehydration as established in our previous study (18). This was attributed to the hygroscopic nature of PVP (34). Our previous investigation using modulated heat-scan and heat-cool-heat scan indicated that water content plays a major role as a plasticizer for PVP filament (18). The T_g of PVP filament (plasticised with TEC) were in much lower range (19-35 °C) than expected from Gordon-Taylor equation ($T_g = 82.3$ °C). However, the T_g obtained in the second heat flow (following water evaporation) was 93 °C.

The addition of budesonide appeared to have a limited effect on the T_g of the filament and the tablet (Fig. 5A). This might be due to the limited concentration of budesonide in the product (2.3%). In case of diclofenac sodium, when same level of plasticization

was initially investigated (12.5%), a brittle filament was produced with a higher T_g (44.89 °C) (Supplementary Data, Fig. S4). In fact, a high level of plasticization (TEC 17.5%) was deemed necessary to produce a compatible filament, this was reflected with a shift of T_g upon the addition of diclofenac sodium to 16.27°C (Fig. 5B). The addition of theophylline on the other hand as reported in our earlier work led to a depression in the T_g of the filament (18). Such a shifts can be attributed to the plasticizing effect of theophylline (35).

The XRPD patterns of budesonide loaded filament and tablets (Fig. 6) exposed the absence of peaks at (2θ) = 6.2, 12.1, 15.5, 16.1, 22.9 indicating no crystalline presence in the PVP matrices (36, 37). For diclofenac sodium, XRPD spectra demonstrated several diffraction peaks at (2θ) = 11.3, 15.3, 23.5 (38). However, the absence of such peaks in the XRPD of the API loaded filament matrix and tablet suggests that the majority of diclofenac sodium remained in the amorphous form. On the other hand, as reported in our earlier study (18) theophylline remained in a crystalline form in the PVP-talc based matrix.

The dissolution pattern of all tested APIs indicated a pH-dependant drug release (Fig. 7A). When these tablets were assessed in more physiologically relevant dissolution medium (28), a slower dissolution pattern was noted (Fig. 7B). Such effect might be related to the lower buffer capacity of bicarbonate buffers in comparison to phosphate based ones (39). The faster drug release of diclofenac sodium in comparison with budesonide might be related to its higher drug loading as well as solubility of (26 mg/mL) (40) in comparison to budesonide (0.0429 mg/mL) (41).

The disintegration test indicated that all tablets remained intact after 1 h in the disintegration medium (Table II). However, upon pH change the disintegration time was significantly longer than the Pharmacopeial standards (9). Such behaviour is related to the nature of core, where polymeric matrices erodes slowly upon exposure to media rather than the exploding of the core in tablets produced by powder compression. The acid uptake behaviour indicated a relatively high acid uptake (Table II). However, these results should be interpreted with caution when compared to coated tablets, where weight gain of 3-7% is usually applied of the enteric coating to achieve protection. In presented example, the shell represents approximately 50% of the tablet total weight.

In summary, by adapting FDM 3D printing to two polymeric matrices and co-ordinating the construction of core and shell structures, the potential of 3D printing technology in fabricating patient-specific pH-responsive tablets has been demonstrated.

CONCLUSION

It was possible to fabricate tablets based on shell-core structure with increasing shell thicknesses using dual FDM 3D printing. Following pH change dissolution test, it was necessary to obtain a shell thickness ≥ 0.52 mm in order to achieve sufficient core protection in the acid medium. To the author's knowledge, this is the first report of producing delayed release tablets based on a 3D printing technology. The process presents a single step production method for gastric-resistant products. This work illustrates the potential of employing dual FDM 3D printing to overcome the rigidity of traditional techniques of manufacturing delayed release solid dosage forms in response to demands from clinical and industrial sectors.

ACKNOWLEDGMENTS

The authors would like to thank UCLAN Innovation Team for their support and Mrs Rim Arafat for her help with graphics design.

REFERENCES

1. Rajjada D, Genina N, Fors D, Wisaeus E, Peltonen J, Rantanen J, Sandler N. A step toward development of printable dosage forms for poorly soluble drugs. *Journal of pharmaceutical sciences*. 2013;102(10):3694-3704.
2. Habib WA, Alanizi AS, Abdelhamid MM, Alanizi FK. Accuracy of tablet splitting: Comparison study between hand splitting and tablet cutter. *Saudi Pharm J*. 2014;22(5):454-459.
3. Peek BT, Al-Achi A, Coombs SJ. Accuracy of tablet splitting by elderly patients. *JAMA*. 2002;288(4):451-452.
4. Noviasky J, Lo V, Luft DD, Saseen J. Clinical inquiries. Which medications can be split without compromising efficacy and safety? *J Fam Pract*. 2006;55(8):707-708.
5. Skowrya J, Pietrzak K, Alhnan MA. Fabrication of extended-release patient-tailored prednisolone tablets via fused deposition modelling (FDM) 3D printing. *European journal of pharmaceutical sciences : official journal of the European Federation for Pharmaceutical Sciences*. 2015;68:11-17.
6. Alhnan MA, Okwuosa TC, Sadia M, Wan KW, Ahmed W, Arafat B. Emergence of 3D Printed Dosage Forms: Opportunities and Challenges. *Pharm Res*. 2016;33(8):1817-1832.
7. Nollenberger K, Albers J. Poly(meth)acrylate-based coatings. *International journal of pharmaceutics*. 2013;457(2):461-469.
8. Sakae O, Hiroyasu K. Application of HPMC and HPMCAS to Aqueous Film Coating of Pharmaceutical Dosage Forms. In: McGinity JW, Felton LA, editors. *Aqueous Film Coating of Pharmaceutical Dosage Forms*. Boca Raton, FL.: CRC Press; 2008.

9. Revision USPCCo. U.S. pharmacopeia & national formulary: United States Pharmacopeial Convention, Inc.; 2007.
10. Katstra WE, Palazzolo RD, Rowe CW, Giritlioglu B, Teung P, Cima MJ. Oral dosage forms fabricated by Three Dimensional Printing™. *Journal of Controlled Release*. 2000;66(1):1-9.
11. Rowe CW, Katstra WE, Palazzolo RD, Giritlioglu B, Teung P, Cima MJ. Multimechanism oral dosage forms fabricated by three dimensional printing (TM). *Journal of Controlled Release*. 2000;66(1):11-17.
12. Yu DG, Yang XL, Huang WD, Liu J, Wang YG, Xu H. Tablets with material gradients fabricated by three-dimensional printing. *Journal of pharmaceutical sciences*. 2007;96(9):2446-2456.
13. Rowe CW, Wang CC, Monkhouse DC. TheriForm Technology. In: Rathbone MJ, Hadgraft J, Roberts MS, editors. *Modified-Release Drug Delivery Technology*, Second Edition. New York: Marcel Dekker Inc; 2003. p. 77-78.
14. Goyanes A, Buanz AB, Hatton GB, Gaisford S, Basit AW. 3D printing of modified-release aminosaliclate (4-ASA and 5-ASA) tablets. *European journal of pharmaceutics and biopharmaceutics : official journal of Arbeitsgemeinschaft fur Pharmazeutische Verfahrenstechnik eV*. 2014.
15. Goyanes A, Buanz ABM, Basit AW, Gaisford S. Fused-filament 3D printing (3DP) for fabrication of tablets. *Int J Pharm*. 2014;476(1-2):88-92.
16. Sandler N, Salmela I, Fallarero A, Rosling A, Khajeheian M, Kolakovic R, Genina N, Nyman J, Vuorela P. Towards fabrication of 3D printed medical devices to prevent biofilm formation. *Int J Pharm*. 2014;459(1-2):62-64.
17. Pietrzak K, Isreb A, Alhnan MA. A flexible-dose dispenser for immediate and extended release 3D printed tablets. *European journal of pharmaceutics and biopharmaceutics : official journal of Arbeitsgemeinschaft fur Pharmazeutische Verfahrenstechnik eV*. 2015.
18. Okwuosa TC, Stefaniak D, Arafat B, Isreb A, Wan KW, Alhnan MA. A Lower Temperature FDM 3D Printing for the Manufacture of Patient-Specific Immediate Release Tablets. *Pharm Res*. 2016.
19. Sadia M, Sosnicka A, Arafat B, Isreb A, Ahmed W, Kellarakis A, Alhnan MA. Adaptation of pharmaceutical excipients to FDM 3D printing for the fabrication of patient-tailored immediate release tablets. *International journal of pharmaceutics*. 2016.
20. Goyanes A, Chang H, Sedough D, Hatton GB, Wang J, Buanz A, Gaisford S, Basit AW. Fabrication of controlled-release budesonide tablets via desktop (FDM) 3D printing. *Int J Pharm*. 2015;496(2):414-420.
21. Melocchi A, Parietti F, Maroni A, Foppoli A, Gazzaniga A, Zema L. Hot-melt extruded filaments based on pharmaceutical grade polymers for 3D printing by fused deposition modeling. *Int J Pharm*. 2016;509(1-2):255-263.
22. Hergel J, Lefebvre S. Clean color: Improving multi-filament 3D prints. *Comput Graph Forum*. 2014;33(2):469-478.
23. Reiner T, Carr N, Radom, #237, M r, #283, ch, Ond, #345, ej, #352, t'ava, Dachsbacher C, Miller G. Dual-color mixing for fused deposition modeling printers. *Comput Graph Forum*. 2014;33(2):479-486.
24. Dudek P. FDM 3D Printing Technology in Manufacturing Composite Elements. In: *Archives of Metallurgy and Materials*; 2013. p. 1415.
25. Goyanes A, Wang J, Buanz A, Martinez-Pacheco R, Telford R, Gaisford S, Basit AW. 3D Printing of Medicines: Engineering Novel Oral Devices with Unique Design and Drug Release Characteristics. *Molecular Pharmaceutics*. 2015;12(11):4077-4084.
26. Yu DG, Williams GR, Wang X, Liu XK, Li HL, Bligh SWA. Dual drug release nanocomposites prepared using a combination of electrospraying and electrospinning. *Rsc Adv*. 2013;3(14):4652-4658.

27. Yang C, Yu DG, Pan D, Liu XK, Wang X, Bligh SWA, Williams GR. Electrospun pH-sensitive core shell polymer nanocomposites fabricated using a tri-axial process. *Acta Biomaterialia*. 2016;35:77-86.
28. Fadda HM, Basit AW. Dissolution of pH responsive formulations in media resembling intestinal fluids: bicarbonate versus phosphate buffers. *Journal of Drug Delivery Science and Technology*. 2005;15(4):273-279.
29. Alhnan MA, Cosi D, Murdan S, Basit AW. Inhibiting the gastric burst release of drugs from enteric microparticles: the influence of drug molecular mass and solubility. *Journal of pharmaceutical sciences*. 2010;99(11):4576-4583.
30. Hao S, Wang B, Wang Y, Zhu L, Wang B, Guo T. Preparation of Eudragit L 100-55 enteric nanoparticles by a novel emulsion diffusion method. *Colloids and Surfaces B: Biointerfaces*. 2013;108:127-133.
31. Thoma K, Bechtold K. Influence of aqueous coatings on the stability of enteric coated pellets and tablets. *European Journal of Pharmaceutics and Biopharmaceutics*. 1999;47(1):39-50.
32. Liu F, Lizio R, Meier C, Peteret HU, Blakey P, Basit AW. A novel concept in enteric coating: a double-coating system providing rapid drug release in the proximal small intestine. *Journal of controlled release : official journal of the Controlled Release Society*. 2009;133(2):119-124.
33. Tudja P, Khan MZ, Mestrovic E, Horvat M, Golja P. Thermal behaviour of diclofenac sodium: decomposition and melting characteristics. *Chem Pharm Bull (Tokyo)*. 2001;49(10):1245-1250.
34. Verdonck E, Schaap K, Thomas LC. A discussion of the principles and applications of Modulated Temperature DSC (MTDSC). *International Journal of Pharmaceutics*. 1999;192(1):3-20.
35. Nair R, Nyamweya N, Gönen S, Martínez-Miranda LJ, Hoag SW. Influence of various drugs on the glass transition temperature of poly(vinylpyrrolidone): a thermodynamic and spectroscopic investigation. *International Journal of Pharmaceutics*. 2001;225(1-2):83-96.
36. Kim JE, Cho HJ, Kim DD. Budesonide/cyclodextrin complex-loaded lyophilized microparticles for intranasal application. *Drug development and industrial pharmacy*. 2014;40(6):743-748.
37. Toropainen T, Velaga S, Heikkila T, Matilainen L, Jarho P, Carlfors J, Lehto VP, Jarvinen T, Jarvinen K. Preparation of budesonide/gamma-cyclodextrin complexes in supercritical fluids with a novel SEDS method. *Journal of pharmaceutical sciences*. 2006;95(10):2235-2245.
38. Korkiatithawechai S, Umsarika P, Praphairaksit N, Muangsin N. Controlled release of diclofenac from matrix polymer of chitosan and oxidized konjac glucomannan. *Mar Drugs*. 2011;9(9):1649-1663.
39. Liu F, Merchant HA, Kulkarni RP, Alkademi M, Basit AW. Evolution of a physiological pH 6.8 bicarbonate buffer system: application to the dissolution testing of enteric coated products. *European journal of pharmaceutics and biopharmaceutics : official journal of Arbeitsgemeinschaft fur Pharmazeutische Verfahrenstechnik eV*. 2011;78(1):151-157.
40. Ming-Thau S, Huei-Lan C, Ching-Cheng K, Cheng-Hsiung L, Sokoloski TD. Dissolution of diclofenac sodium from matrix tablets. *International Journal of Pharmaceutics*. 1992;85(1):57-63.
41. Bhatt H, Naik B, Dharamsi A. Solubility Enhancement of Budesonide and Statistical Optimization of Coating Variables for Targeted Drug Delivery. *Journal of Pharmaceutics*. 2014;2014:13.

List of Tables

Table I Summary of the compositions of API loaded filament and residual drug contents following HME and dual FDM 3D printing.

Table II Summary of gastric resistant properties of 3D printed enteric tablets.

List of Figures

Fig.1 Schematic illustration of the fabrication of 3D-printed shell-core enteric tablet. **(A)** Two complementary stereolithographic files are designed *via* CAD software to create a shell-core structure **(B)** Dual FDM 3D printer is employed with two different filaments; i) filament for enteric shell (based on Eudragit L), and ii) filament core (based API, PVP) processed through HME compounder. A lubricating station is installed for PVP to facilitate the printing of the core during nozzle alternation. **(C)** Image of the 30% completed FDM 3D printer Shell-core.

Fig. 2 (A and B) Rendered images (Autodesk 3DS Max) of shell-core designs with increasing shell thickness (0.17, 0.35, 0.52, 0.70 and 0.87mm), **(C)** Images of 30% completed shell-core designs with theophylline core and increasing Eudragit L100-55 shell thickness, **(D)** SEM images of the surface of the tablets **(E)** Impact of shell thickness of 3D printing on *in vitro* release pattern of theophylline from 3D printed tablet in USP II pH change dissolution test.

Fig. 3 (A) Images of 3D printed enteric theophylline tablet printed with low, medium and higher resolution, **(B)** Impact of resolution of 3D printing on *in vitro* release pattern of theophylline from 3D printed tablet in USP II pH change dissolution test. **(C)** Impact of filler (TBP or talc) on the *in vitro* release pattern of theophylline from 3D printed tablets in USP II pH change dissolution test in phosphate buffer, **(D1,2)** SEM and Raman images (respectively) of a cross-sections of 0.52 mm thickness shell theophylline table.

Fig. 4 TGA thermal degradation profiles of TEC, PVP, PVP:TEC filament, API-free and API loaded filaments, and 3D printed tablets for **(A)** budesonide and **(B)** diclofenac sodium.

Fig. 5 Reversing DSC thermographs of PVP, PVP: TEC filament, API-free and API-loaded filaments, and 3D printed tablets for budesonide **(A1** first heat-scan and **A2** second heat-scan) and diclofenac sodium **(B1** first heat-scan and **B2** second heat-scan).

Fig. 6 XRPD patterns of PVP, PVP: TEC filament, API-free and API-loaded filaments, and 3D printed tablets for **(A)** budesonide and **(B)** diclofenac sodium.

Fig. 7 *In vitro* release pattern of APIs; budesonide, diclofenac sodium or theophylline from 3D printed tablets using a USP II pH change dissolution test in **(A)** phosphate buffer and **(B)** bicarbonate buffer.

Supplementary data

Fig. S1 Impact of lubricants on **(A)** TGA thermal degradation profiles of PVP filament and **(B)** the *in vitro* release pattern of theophylline from core.

Fig. S2 DSC thermographs of Eudragit L100-55, TEC and talc (raw materials), filament and 3D printed shell.

Fig. S3 TGA thermal degradation profiles of the raw materials of; theophylline, PVP, TBP, TEC as well as the physical mixture, the filament and the 3D printed tablets.

Fig. S4 Reversing DSC thermographs of PVP, PVP: TEC (12.5%) filament, as well as diclofenac-loaded filaments (first heat-scan).

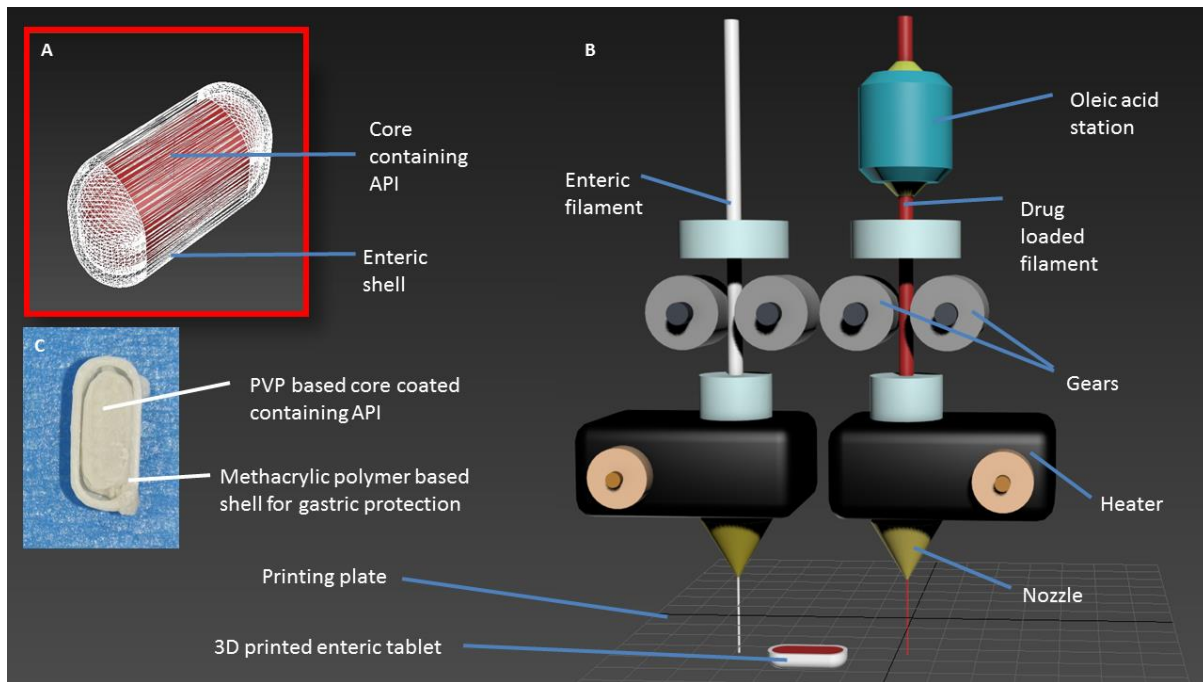


Fig.1 Schematic illustration of the fabrication of 3D-printed shell-core enteric tablet. (A) Two complementary stereolithographic files are designed *via* CAD software to create a shell-core structure (B) Dual FDM 3D printer is employed with two different filaments; i) filament for enteric shell (based on Eudragit L), and ii) filament core (based API, PVP) processed through HME compounder. A lubricating station is installed for PVP to facilitate the printing of the core during nozzle alternation. (C) Image of the 30% completed FDM 3D printer Shell-core.

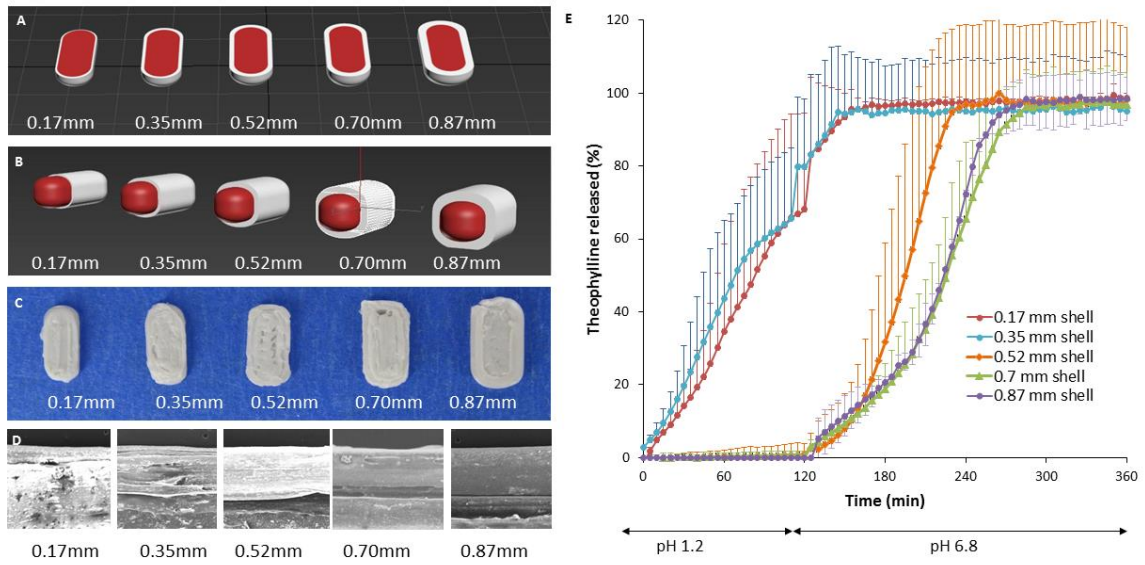


Fig. 2 (A and B) Rendered images (Autodesk 3DS Max) of shell-core designs with increasing shell thickness (0.17, 0.35, 0.52, 0.70 and 0.87mm), **(C)** Images of 30% completed shell-core designs with theophylline core and increasing Eudragit L100-55 shell thickness, **(D)** SEM images of the surface of the tablets **(E)** Impact of shell thickness of 3D printing on *in vitro* release pattern of theophylline from 3D printed tablet in USP II pH change dissolution test.

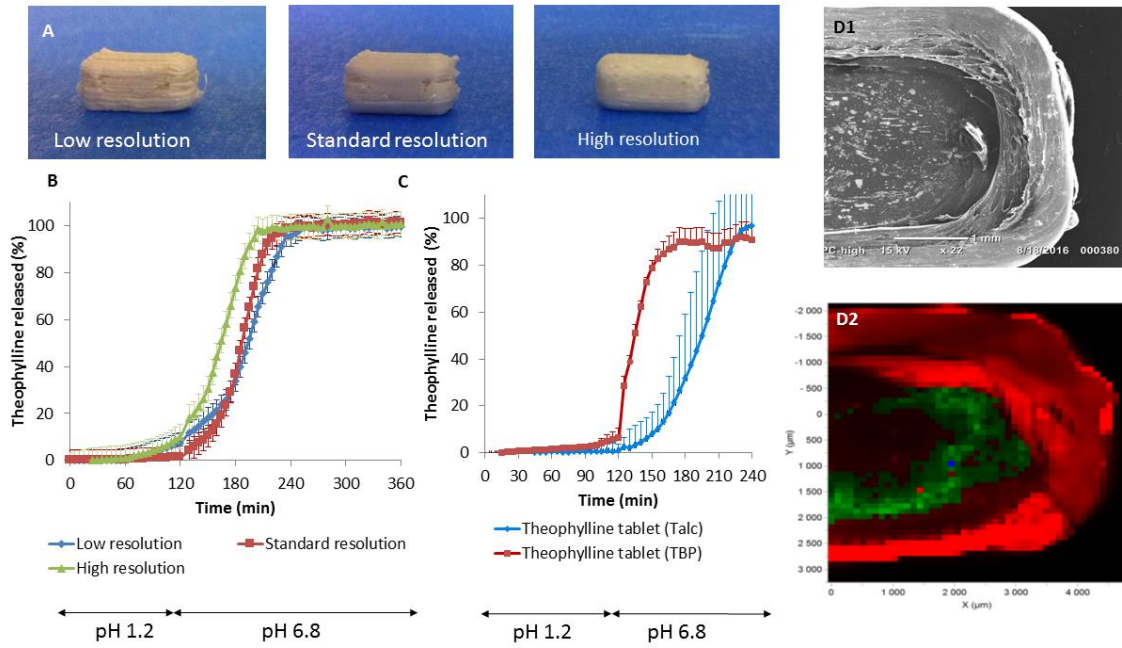


Fig. 3 (A) Images of 3D printed enteric theophylline tablet printed with low, medium and higher resolution, (B) Impact of resolution of 3D printing on *in vitro* release pattern of theophylline from 3D printed tablet in USP II pH change dissolution test. (C) Impact of filler (TBP or talc) on the *in vitro* release pattern of theophylline from 3D printed tablets in USP II pH change dissolution test in phosphate buffer, (D1,2) SEM and Raman images (respectively) of a cross-sections of 0.52 mm thickness shell theophylline table.

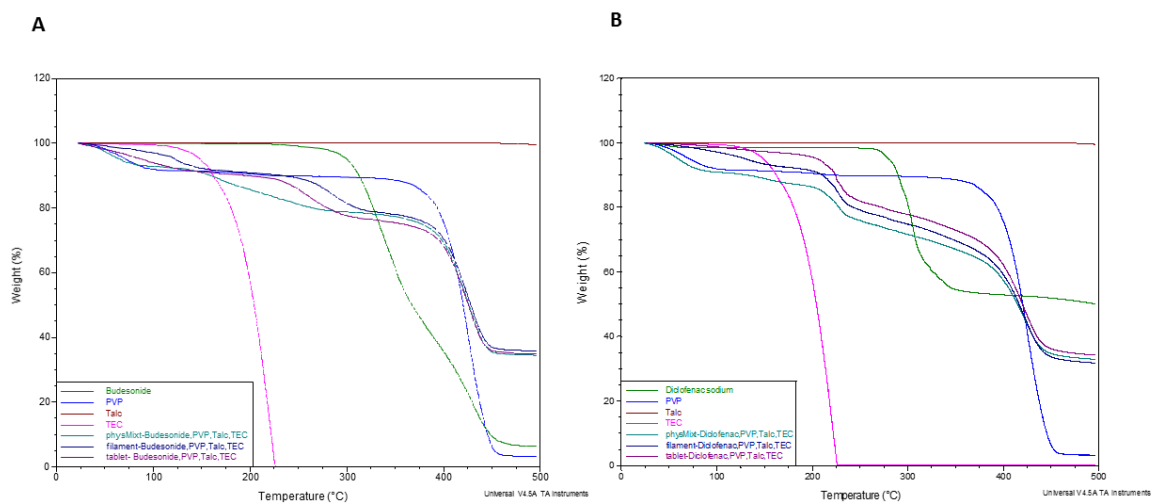


Fig. 4 TGA thermal degradation profiles of TEC, PVP, PVP:TEC filament, API-free and API loaded filaments, and 3D printed tablets for **(A)** budesonide and **(B)** diclofenac sodium.

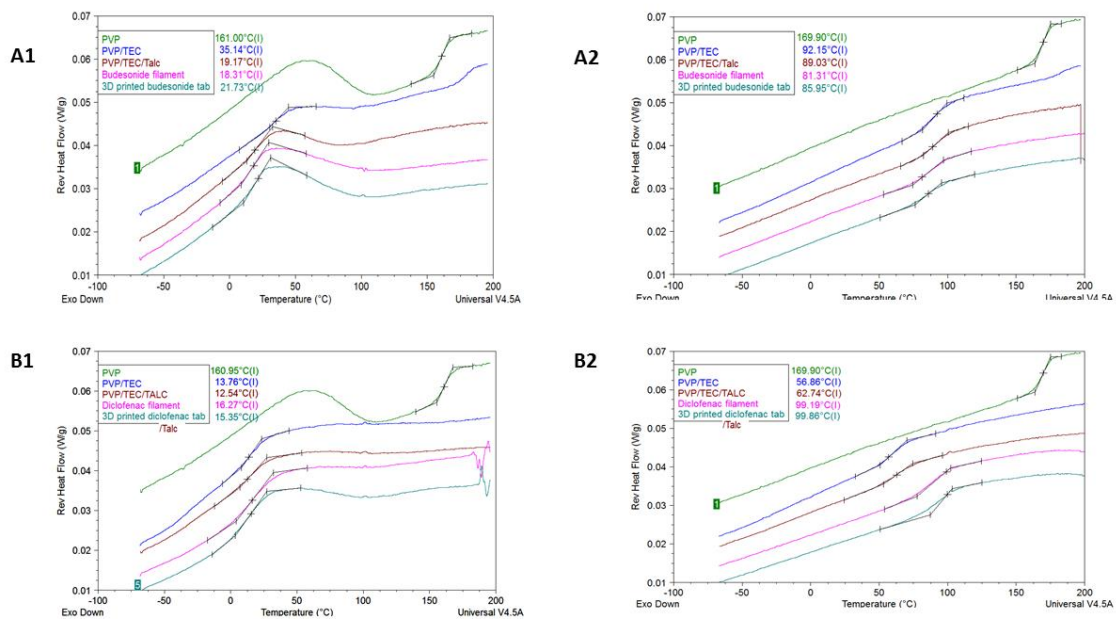


Fig. 5 Reversing DSC thermographs of PVP, PVP: TEC filament, API-free and API-loaded filaments, and 3D printed tablets for budesonide (**A1** first heat-scan and **A2** second heat-scan) and diclofenac sodium (**B1** first heat-scan and **B2** second heat-scan).

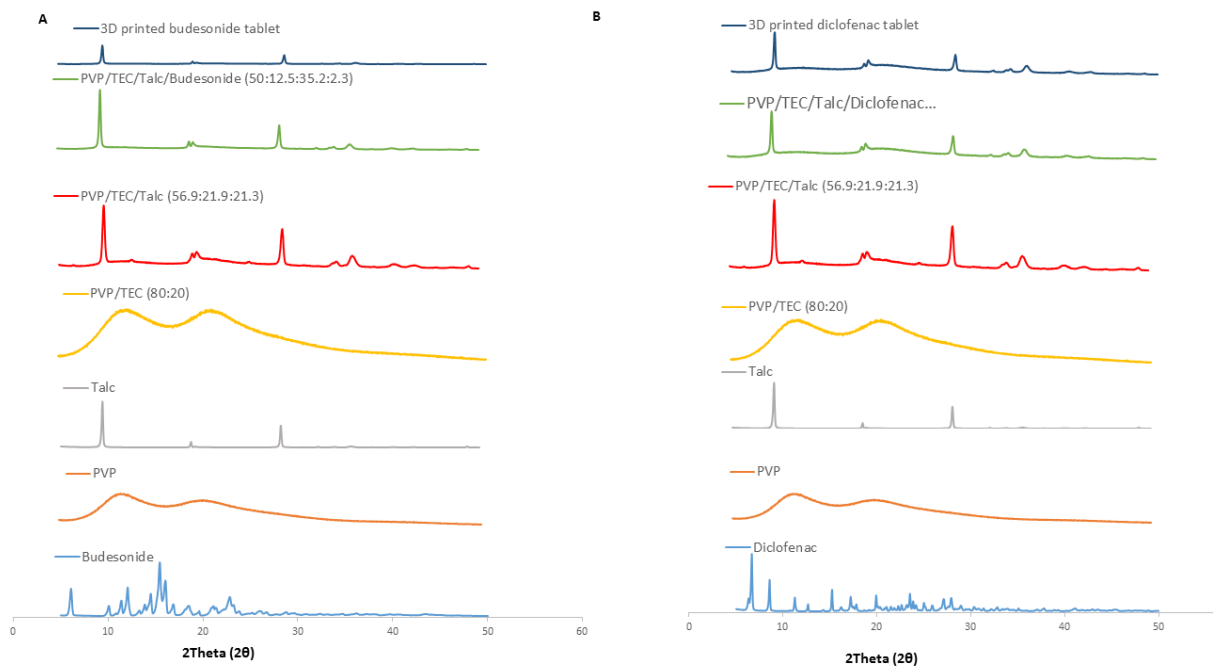


Fig. 6 XRPD patterns of PVP, PVP: TEC filament, API-free and API-loaded filaments, and 3D printed tablets for **(A)** budesonide and **(B)** diclofenac sodium.

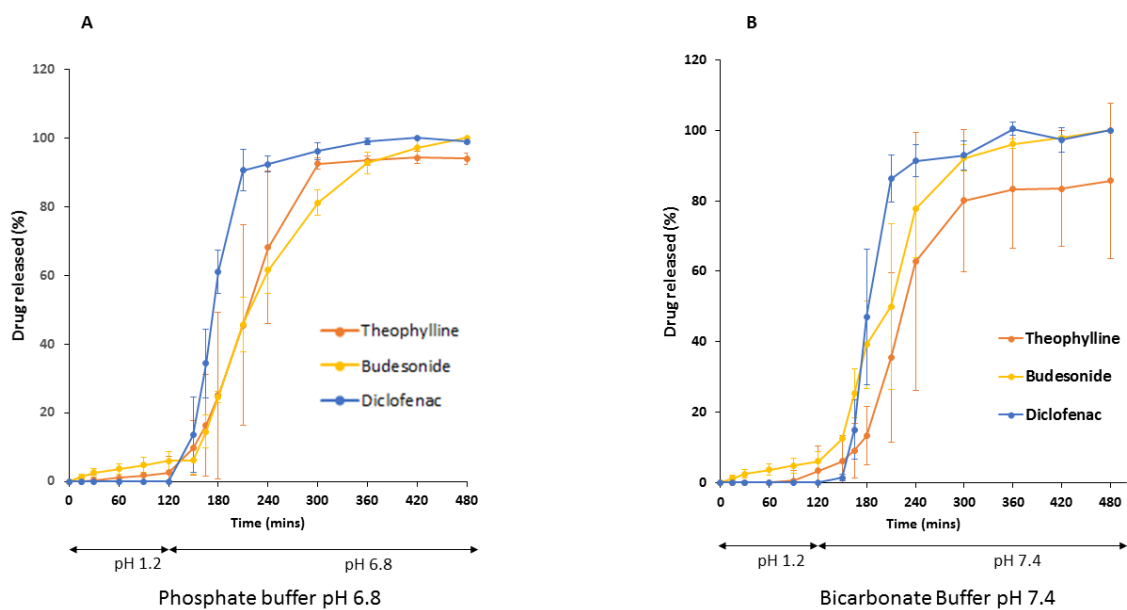


Fig. 7 *In vitro* release pattern of APIs; budesonide, diclofenac sodium or theophylline from 3D printed tablets using a USP II pH change dissolution test in **(A)** phosphate buffer and **(B)** bicarbonate buffer.

Fabricating a Shell-Core Delayed Release Tablet Using Dual FDM 3D Printing for Patient-Centred Therapy

Supplementary data

Tochukwu C Okwuosa¹, Beatriz Pereira¹, Basel Arafat¹, Milena Cieszynska¹, Abdullah Isreb¹, Mohamed A Alhnan^{1*}

¹ School of Pharmacy and Biomedical Sciences, University of Central Lancashire, Preston, Lancashire, UK

*Corresponding author: MAIbedAlhnan@uclan.ac.uk

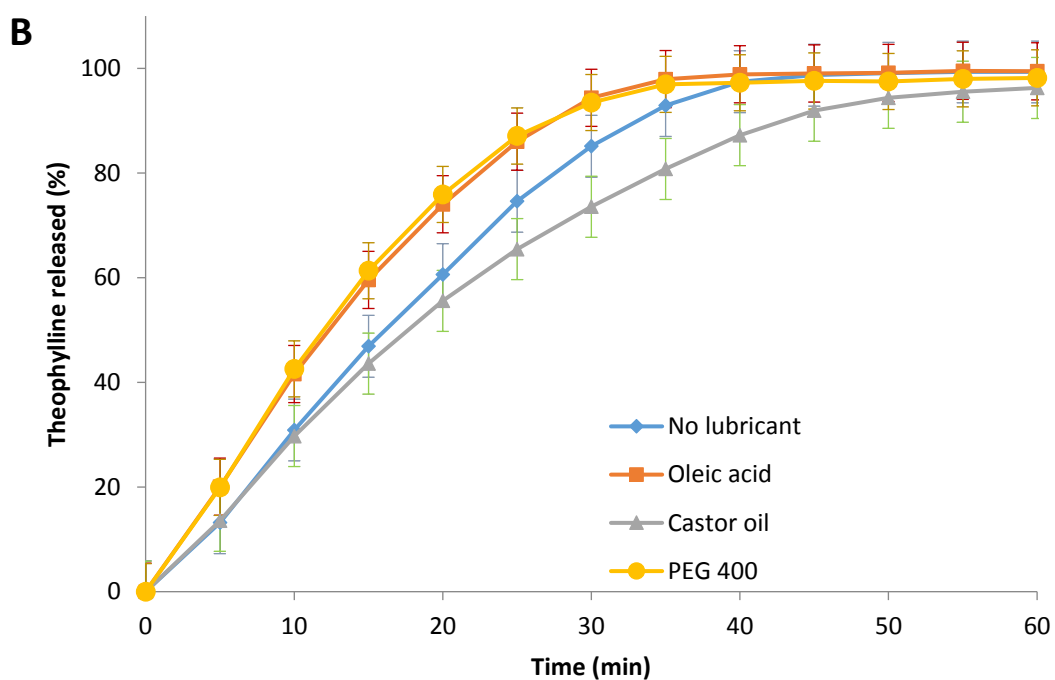
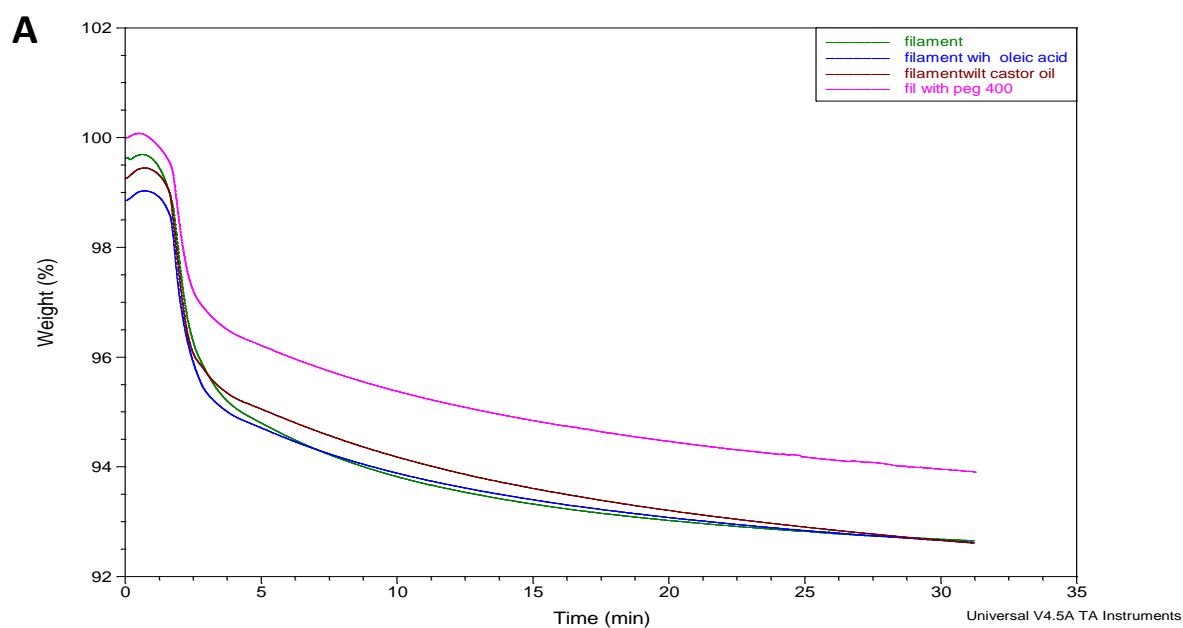


Figure S1 Impact of lubricants on (A) TGA thermal degradation profiles of PVP filament and (B) the *in vitro* release pattern of theophylline from core.

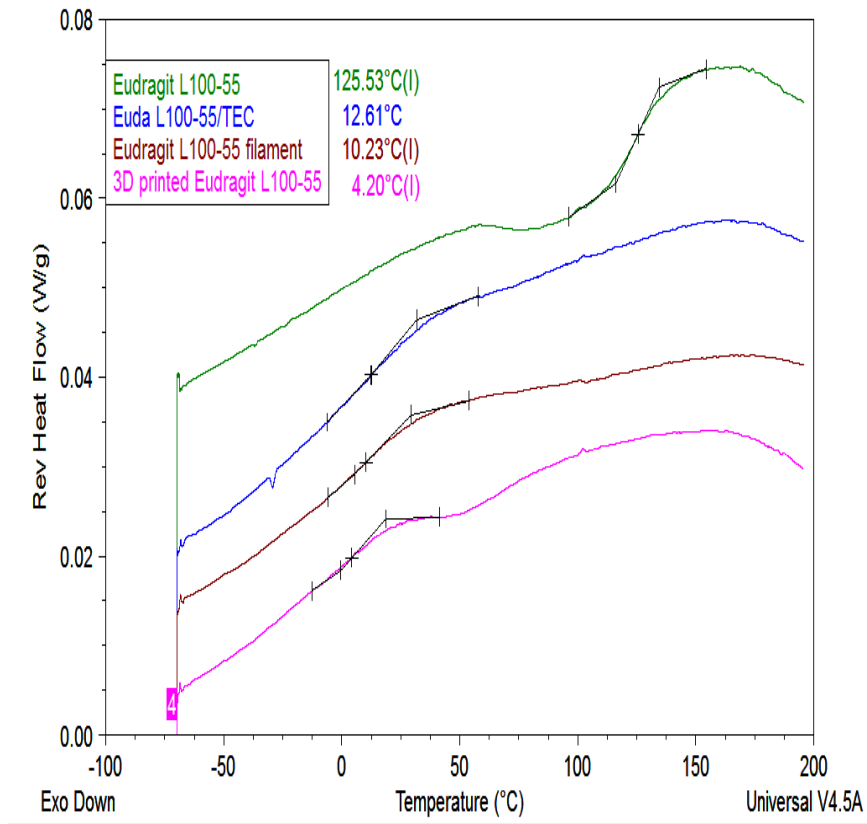


Figure S2 DSC thermographs of Eudragit L100-55, TEC and talc (raw materials), filament and 3D printed shell.

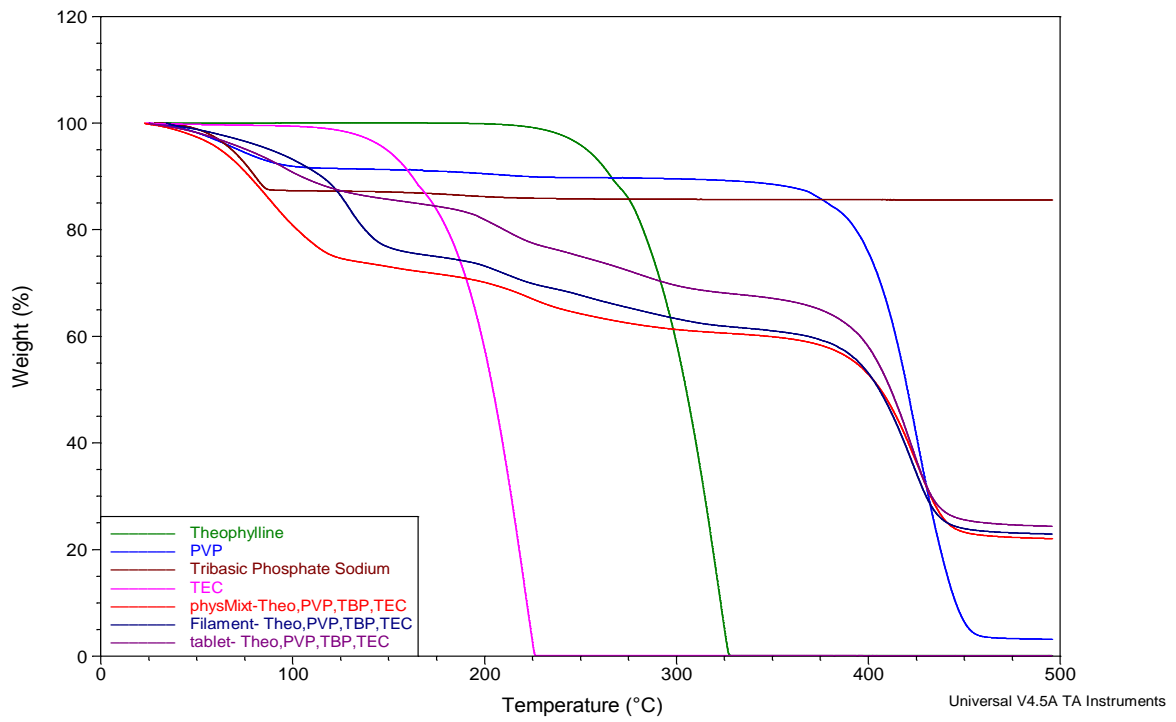


Figure S3 TGA thermal degradation profiles of the raw materials of; theophylline, PVP, TBP, TEC as well as the physical mixture, the filament and the 3D printed tablets.

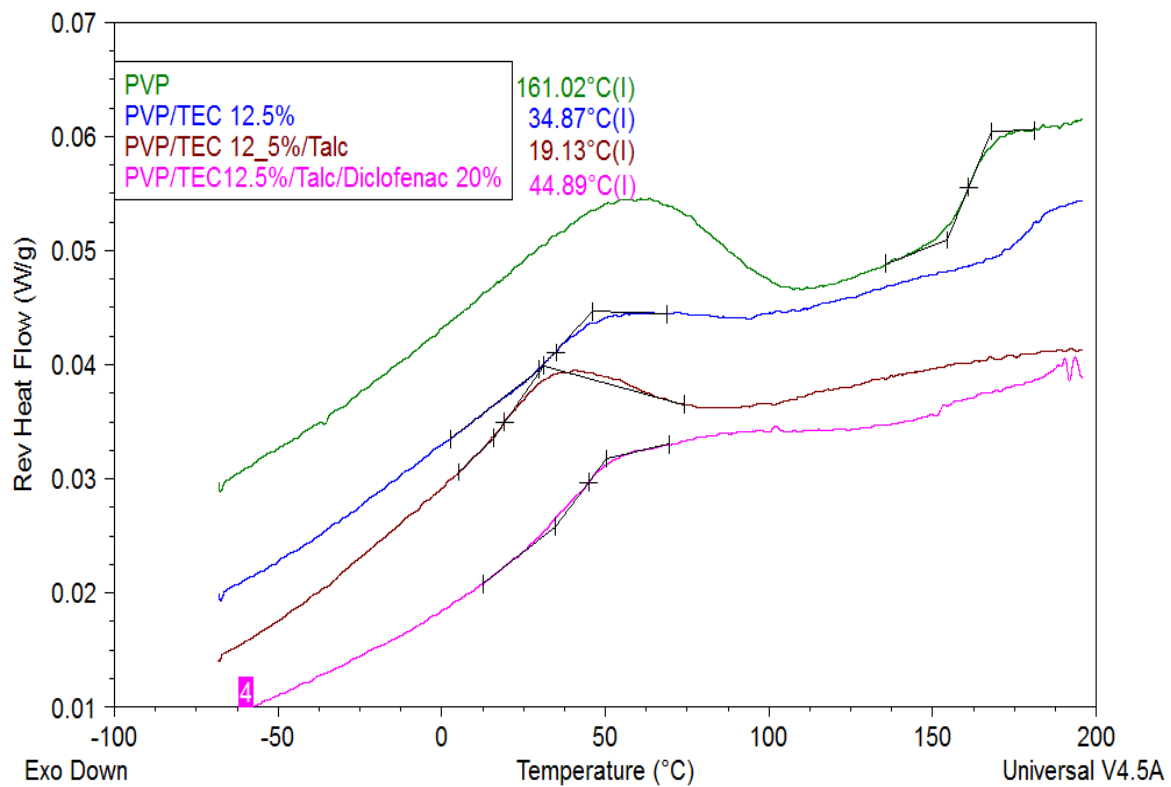


Figure S4 Reversing DSC thermographs of PVP, PVP: TEC (12.5%) filament, as well as diclofenac-loaded filaments (first heat-scan).